



Removal of COD from real oily wastewater by electrocoagulation using a new configuration of electrodes

Muhammad Aiyd Jasim · Forat Yasir AlJaberi

Received: 14 December 2022 / Accepted: 17 April 2023 / Published online: 9 May 2023
© The Author(s), under exclusive licence to Springer Nature Switzerland AG 2023

Abstract In order to bring the chemical oxygen demand (COD) concentration down to safe levels for widespread use, this study plans to use a state-of-the-art electrocoagulation reactor (ECR) to treat real oily wastewater discharged from the Al-Muthanna petroleum refinery. A one-side finned (1SF) cathode tube was positioned between two tubular anodes in the continuous ECR, where the active area of the cathode was much more than its submerged volume. Each of these electrodes was made of aluminum and joined in a monopolar parallel to a DC power supply. On COD elimination efficiency, the impacts of operational parameters such as electrolysis time (4–60 min), current density (0.630–5.000 mA/cm²), and flow rate (50–150 ml/min) were explored. In conclusion, Increasing current density and electrolysis duration increases COD removal efficiency, whereas increasing flow rate reduces it. COD removal efficiencies were 82% at optimal electrolysis times of 60 (min), 5 (mA/cm²) current density, and 50 (ml/min) flow rate, with energy consumption of 4.787 (kWh/kg_{COD}) and electrode consumption of 0.544 (g). The

investigation results demonstrated that the new reactor could treat oily wastewater within the specified operational limits. It might be used before other, more conventional treatments.

Keywords Real oily wastewater · Electrocoagulation · Energy consumption · Electrode consumption · One-sided finned cathode (1SF) · Monopolar-parallel connection

Introduction

Oil is a vital economic resource for many nations due to the wide range of industries that rely on it and its byproducts. This includes the petrochemical and oil refining sectors (AlJaberi et al., 2020). During oil production, vast quantities of oily wastewater are discharged (Hassan et al., 2018). Oily wastewater from drilling sites, refineries, and petrochemical plants degrade the environment (Changmai et al., 2019). Releasing untreated or partially treated wastewater from petroleum refineries has adverse effects on the environment and wildlife, including contamination of amphibian biological systems, unwanted ecological difficulties, expensive effluent treatment, and a scarcity of farmland and fish (Mustapha, 2018). Oily wastewater treatment and reuse are crucial to the environmentally sustainable management of oil-producing zones and the economic growth of the petrochemical sector (Mohammed & AlJaberi, 2021; Yang et al., 2021).

M. A. Jasim (✉)
Chemical Engineering Department, College
of Engineering, Al-Qadisiyah University, Al-Qadisiyah,
Iraq
e-mail: Eng.chem21.post13@qu.edu.iq

F. Y. AlJaberi (✉)
Chemical Engineering Department, College
of Engineering, Al-Muthanna University, Samawah,
Al-Muthanna, Iraq
e-mail: furat_yasir@yahoo.com

Biochemical oxygen demand (BOD), total suspended solids (TSS), chemical oxygen demand (COD), total organic carbon (TOC), total dissolved solids (TDS), turbidity (TUR), ammonia, cyanide, and heavy metals are all examples of organic and inorganic components found in crude oil there is a wide range of oil concentrations in wastewater, from 1 to 40,000 parts per million, which is discharged annually in the form of billions of cubic meters (Ahmed et al., 2020). Thus, oily wastewater drained into the ocean is the primary cause of ecological damage to the ocean (Changmai et al., 2019). There is between 0.4 and 0.6% oily wastewater in crude oil (Jiang et al., 2019). The resources, shapes, consequences, and remedial advantages of oily wastewater are depicted in Fig. 1 (Mokif et al., 2022).

Human health can be negatively impacted by oily wastewater because it is difficult to degrade. Therefore, different effluent sources require different treatments based on the amount and type of emulsified oily waste (Jabbar et al., 2020). This objective is treatable by cyclone separation, sorption, chemical precipitation, and electrochemical methods (Cheng & Gong, 2018). Removal capacity, treatment interaction time, optional pollutants created, building cost, and unit operation/maintenance determine the success of the applied procedures. Because of the growing expansion of industry and human requirements, a clever COD reduction method from

wastewater and freshwater reuse is required (Ghanbari & Moradi, 2016). Wastewater discharge standard limit (COD < 100 mg/l) (Jain & Singh, 2003).

Electrochemical techniques such as electro-oxidation, electro-floatation, and electro-Fenton are extensively employed to treat many types of wastewater due to their ease of automation and application (AlJaberi, 2018). Electrocoagulation (EC) is a good way to clean oily wastewater deeply with electrochemical treatment. Redox processes are utilized in EC and occur when an electric current is transmitted between electrodes, which are often made of aluminum or iron. The cathode is the reduced electrode, and the anode is the oxidized one. As shown schematically in Fig. 2, aluminum cations (Al^{+3}) released as a result of anode degeneracy create electro-coagulants ($Al(OH)_3$). Both hydrogen gas (H_2) and hydroxyl ions (OH^-) are generated at the cathode of an EC cell (Al-Zuheri & Mohammed, 2018; Almkudad et al., 2021).

The rate of organic and inorganic pollutant removal is strongly dependent on the amount of metal (electrode dissolve) that increases the electrocoagulation process's overall treatment efficacy. Anode disintegration increases metal cation concentrations, such as Al^{3+} or Fe^{2+} , whereas the cathode generates hydrogen gas (H_2) and hydroxyl ions (OH^-) (Barzega et al., 2019; Papadopoulos et al., 2019). Different ions produced at both electrodes form electro-coagulants, which remove pollutants via adsorption without

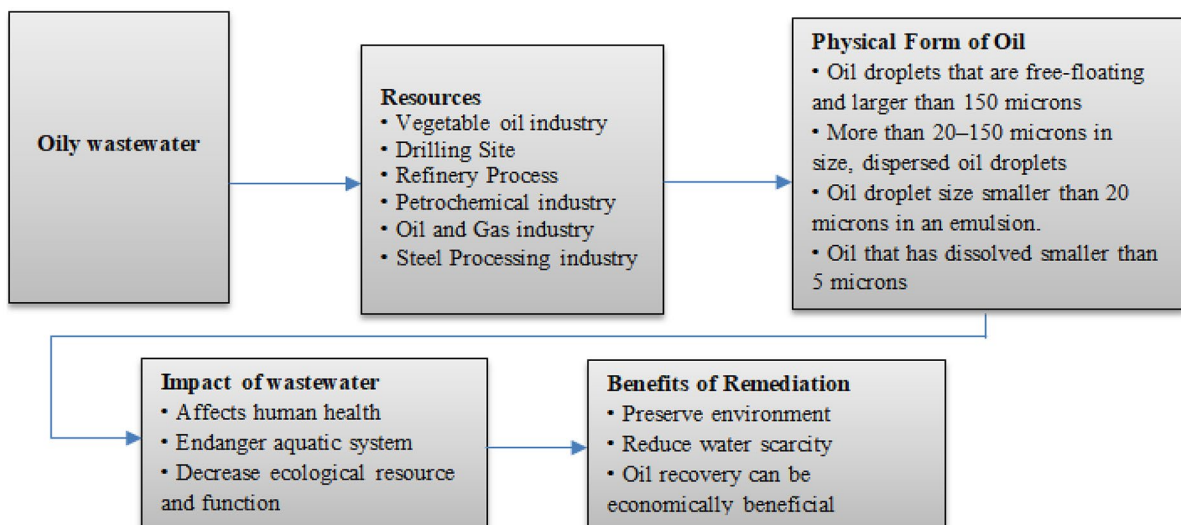


Fig. 1 General diagram for oily wastewater sources, effects, physical forms, and advantages of remediation

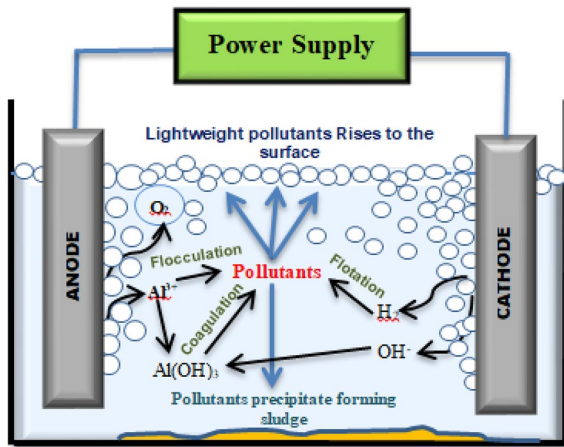
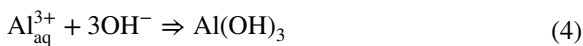
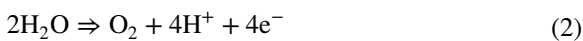


Fig. 2 Schematic illustration of a fundamental EC cell

chemical additives (de Carvallho et al., 2015). Electro coagulants, such as Al(OH)_3 , are produced by chemical interactions between different ions (Eqs. 1–5) (AlJaberi et al., 2020).



The electro-coagulants produced through electrocoagulation, namely Al(OH)_3 , are more effective than chemical coagulants at removing pollutants from different types of wastewater. Similarly, they are more significant than chemical coagulants, resulting in minimal solubility within a specific pH range where they will rapidly separate (Jabbar et al., 2020). The metal, shape, arrangement of the electrodes, the mode of operation (batch or continuous), and the AC/DC supply all influence the design of electrocoagulation reactors (Mohammed & AlJaberi, 2018).

In this study, natural oily wastewater is treated using a continuous electrocoagulation reactor (ECR) to reduce COD and meet environmental laws. The aluminum electrodes in an (ECR) are positioned

Table 1 Real-world oily wastewater characterization

Parameters	Value
Oil content (ppm)	1870.41
COD (ppm)	1320
TDS (ppm)	2150
Conductivity ($\mu\text{s/cm}$)	4267
pH	8.1
Temperature ($^\circ\text{C}$)	25

concentrically and wired to a DC power source in a monopolar-parallel configuration. The cathode was designed as a one-sided finned (1SF) cylindrical form that sits between the anodes, whereas an anode has a plane-cylindrical shape.

Recent research has focused on developing more effective electrocoagulation cells, as discussed in the review articles. However, studies have yet to be conducted on treating natural oily wastewater in an electrocoagulation reactor with tubular aluminum anodes encircling a one-sided finned (1SF) cylindrical aluminum cathode. Consequently, this research aims to use this unique reactor to lower the amount of chemical oxygen demand (COD) in the oily wastewater produced by the Al-Muthanna petroleum refinery and to quantify the energy and electrode consumption of this new method while adjusting for optimal operating factors (the applied current and reaction time). For experimental design, analysis, and optimization, the response surface methodology-central composite design (RSM-BBD) experimental design approach and the Minitab soft software were used.

Materials and methods

Natural oily wastewater characterization

Natural oily wastewater was taken from the downstream end of Al-Muthanna petroleum refinery wastewater and preserved at 4°C until a continuous electrocoagulation reactor was used, as shown in Table 1. According to statistics supplied by the refinery’s management, the quantity of wastewater created by this plant daily was around $25 \text{ m}^3/\text{day}$.

Equation 6 was used to compute the percentage pollutants removal efficiency (Y) as follows (AlJaberi, 2020):

$$Y\% = \frac{C_i - C_f}{C_i} \times 100\% \quad (6)$$

C_i and C_f are the concentrations of the pollutant at the beginning and end, in mg/l. Furthermore, the following equations were used to determine the theoretical consumption of electrodes (TCE), the actual consumption of electrodes (ACE), and the electrical energy consumption (EEC) of the continuous electrocoagulation process (Ahmed et al., 2020):

$$EEC = \frac{U I t * 1000}{(C_i - C_f) * V} \quad (7)$$

where U represents the operating voltage (volt), I represents the applied current (Ampere), t is the electrolysis period (hours), and V represents the sample volume (liter) (AlJaberi et al., 2020).

$$TCE = \frac{I t M}{Z F} \quad (8)$$

where Z represents the number of electrons (for Al, it is 3), M represents the molecular weight of the electrodes' metal (26.98 g/mol), and F represents the Faraday constant (96,485.34 Columb/mol).

$$ACE = W_1 - W_2 \quad (9)$$

where W_1 represents the weight of the electrodes before the experiment, and W_2 represents the weight of the electrodes following the experiment. We may determine the current efficiency value by comparing the theoretical and real electrode consumption numbers, as shown in Eq. (10) (AlJaberi, 2019):

$$\text{Current efficiency} = (ACE/TCE) * 100\% \quad (10)$$

Electrocoagulation reactor

We employed DC power to maintain a constant current and allow real-time voltage changes (YX-305D, Yaxun, China). The electric flocculation tank was made of plastic and had a capacity of 2.5 l. The current study used an electrocoagulation reactor (Fig. 3) with three concentric electrodes made of aluminum tubes. The two tubes on each end were the anode electrodes, while the middle tube was the cathode. The physical composition of anode tubes was analyzed by EDS (energy-dispersive X-ray spectroscopy), which showed that the tubes include a wide range of chemicals. Table 2 and Fig. 4 show that the cathode is an aluminum one-side finned (1SF) tube with a surface area of 2185 cm², dimensions of 3.4 cm by 8.8 cm, and 27 fins with a diameter of 2.5 cm by 8.8 cm. Tubular aluminum anodes surround the cathode with dimensions of (an outer anode of 12 cm 10 cm and an inner anode of 1.5 cm 10 cm) with a total surface area of 425 cm². These electrodes were submerged at a height of 7.5 cm when the wet volume was substantially smaller than the active area of the anodes. Wet volume here refers to the anodes' submerged area.

The obtained active area of 319 cm² was much more than the submerged volume of 861 cm³. The outer anode was 2 cm from the finned-side cathode, whereas the inner anode was 1 cm from the non-finned-side cathode. The electrocoagulation reactor's core had

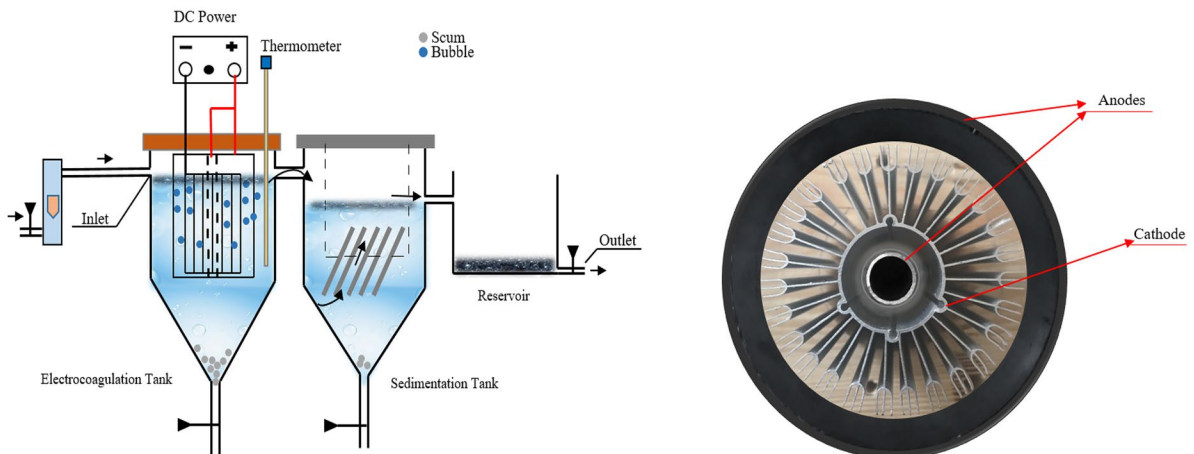


Fig. 3 A diagram depicting the electrocoagulation cell and electrode layout

Table 2 Aluminum tube characterization

Element	Weight %
C	17.9
O	7.1
Na	0.1
Al	73.4
Si	0.2
S	0.1
Cl	0.2
Ca	0.3
Fe	0.6

these electrodes powered by an electrical source (0–30 V and 0–5 Amps). Figure 3 shows the electrocoagulation reactor and electrodes. This study examined COD. After each experiment, the electrodes were cleaned with sandpaper, washed with distilled water, dried, and weighed. The pH was measured using a digital pH meter (HNNA Instrument Inc, PH211, Romania). In contrast, an electronic conductivity and TDS meter were used to measure the conductivity and TDS (HM digital meter, model COM-100, Korea). Samples were collected, and COD values were determined using a thermos-reactor (RD-125, Lovibond) and a spectrophotometer (MD 200, Lovibond).

Experimental design

The electrocoagulation experiments were designed, analyzed, and optimized using response surface methodology (RSM) type Box-Behnken design (BBD) and a statistical program (Minitab-18). The mathematical connection between the responses and the operational variables is approximated by putting

Table 3 Operating experimental variable ranges

Real variables (X_i)	Coded variables		
	-1	0	+1
X_1 : CD (mA/cm ²)	0.630	2.815	5.000
X_2 : Electrolysis time (min)	4	32	60
X_3 : Flow rate (ml/min)	50	100	150

the replies into a second-order polynomial equation (Eq. 6). The higher the regression coefficient (R^2) value, as well as the results of the analysis of variance (ANOVA), the higher the quality of the model constructed (AlJaberi, 2018; Mohammed & AlJaberi, 2018):

$$Y = B_{0+} + \sum_{i=1}^q B_i X_i + \sum_{i=1}^q B_{ii} X_i^2 + \sum_i \sum_j B_{ij} X_i X_j \quad (11)$$

where X_1, X_2, \dots, X_q are the operational variables, q is the total number of operating variables, B_o to B_{ij} are the regression coefficients, and Y is the researched answers, labeled as $Y_{COD\%}$ for chemical oxygen demand removal efficiency.

In the current work, the influences of current density CD (X_1 : 0.630–5.00 mA/cm²), electrolysis time (X_2 : 4–60 min), and the flow rate (X_3 : 50–150 ml/min) were investigated.

Design specialists offered 12 experiments with 3 center points, i.e., using RSM kind Box-Behnken design BBD with the Minitab statistical software program, to optimize the observed responses, namely chemical oxygen demand (COD) elimination. The study designs and experimental ranges for the operational variables are mentioned respectively in Tables 3 and 4.

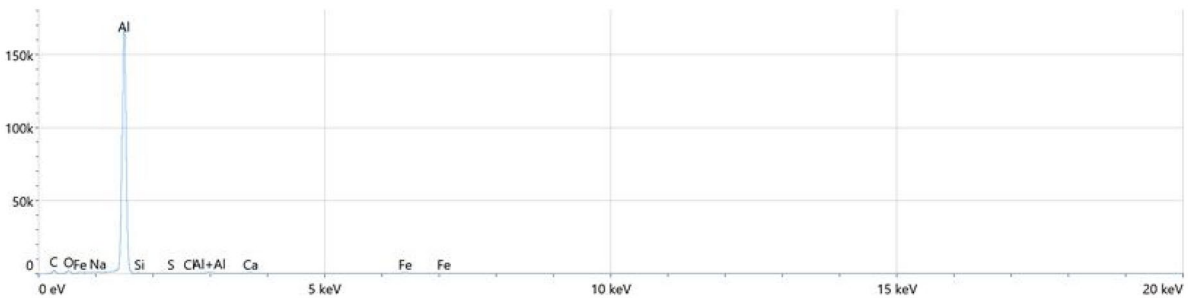


Fig. 4 Energy-dispersive detectors (EDS) of aluminum tube

Table 4 Experiments design

Run	X_1 : coded value	X_2 : coded value	X_3 : coded value	X_1 : CD (mA/cm ²)	X_2 : electrolysis time (min)	X_3 : flow rate (ml/min)
1	-1	-1	0	0.630	4	100
2	+1	-1	0	5.000	4	100
3	-1	+1	0	0.630	60	100
4	+1	+1	0	5.000	60	100
5	-1	0	-1	0.630	32	50
6	+1	0	-1	5.000	32	50
7	-1	0	+1	0.630	32	150
8	+1	0	+1	5.000	32	150
9	0	-1	-1	2.815	4	50
10	0	+1	-1	2.815	60	50
11	0	-1	+1	2.815	4	150
12	0	+1	+1	2.815	60	150
13	0	0	0	2.815	32	100
14	0	0	0	2.815	32	100
15	0	0	0	2.815	32	100

Results and discussion

Table 5 shows the theoretical and practical COD removal efficiencies, tubular electrode usage, and current efficiency. As shown in Fig. 5, the observed range for COD elimination is 3.03–77.58%, which agrees well with the projected range of 4.18–76.43%.

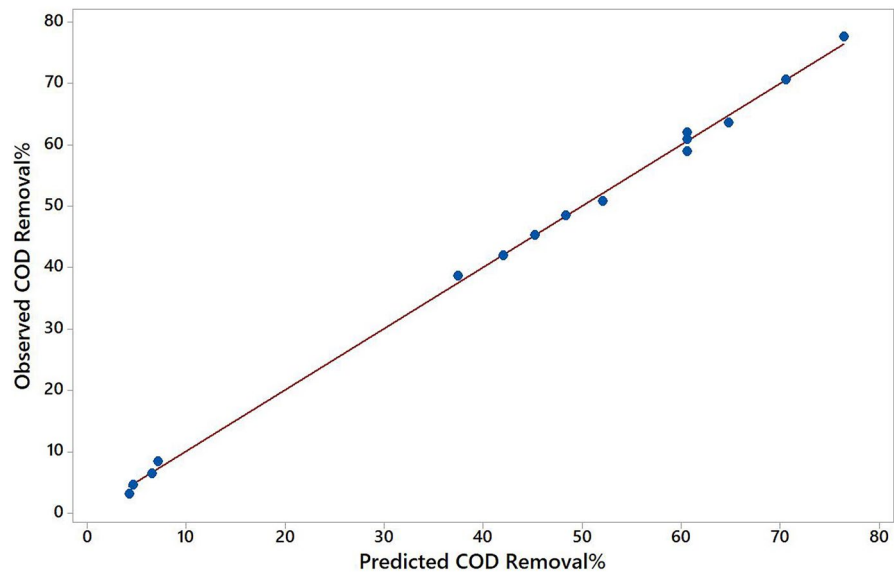
Mathematical relation of the investigated responses

Based on experimental data, the mathematical correlation (Eq. 12) in Table 6 depicts the interactions between operational factors in terms of actual parameters that impact COD removal efficiency. As said, COD models with high regression parameters and

Table 5 The investigated variables' results

Run	X_1 : CD (mA/cm ²)	X_2 : electrolysis time (min)	X_3 : flow rate (ml/min)	Experimental $Y_{\text{COD}\%}$	Predicted $Y_{\text{COD}\%}$	Theoretical consumption (g)	Actual consumption (g)	Ec (kWh/kg _{COD})
1	0.630	4	100	4.55	4.59	0.005	0.011	0.15
2	5.000	4	100	8.33	7.07	0.036	0.011	2.00
3	0.630	60	100	50.76	52.02	0.070	0.140	0.19
4	5.000	60	100	70.61	70.56	0.547	0.210	3.88
5	0.630	32	50	48.41	48.30	0.038	0.100	0.11
6	5.000	32	50	63.56	64.75	0.290	0.180	2.25
7	0.630	32	150	38.64	37.44	0.036	0.080	0.12
8	5.000	32	150	41.89	42.01	0.288	0.130	3.30
9	2.815	4	50	6.44	6.51	0.020	0.021	0.93
10	2.815	60	50	77.58	76.43	0.302	0.280	1.21
11	2.815	4	150	3.03	4.18	0.020	0.020	2.01
12	2.815	60	150	45.23	45.16	0.312	0.130	2.12
13	2.815	32	100	58.86	60.58	0.165	0.170	0.85
14	2.815	32	100	60.91	60.58	0.165	0.160	0.82
15	2.815	32	100	61.97	60.58	0.165	0.160	0.80

Fig. 5 Predicted and observed values for chemical oxygen demand %



excellent agreement with adjusted response values are desirable (Schaep et al., 1998).

Analysis of variance (ANOVA)

The Pareto diagram offered in Fig. 6 depicted the factors, the square of the factors, the most active interventions, and their interactions on the COD removal effectiveness response. The electrolysis period has the most impact, and then the electrolysis duration square is, respectively, according to the shape.

Analysis of variance (ANOVA) is used to evaluate the model fitted. Hence, it was used to fit the function to the data. If the models are not well specified, the findings may be deceptive (Ahmed et al., 2020; AlJaberi, 2020).

Influence of process parameters on the efficiency of COD removal The analysis of variance for COD removal efficiency is shown in Table 7, with values less than 0.050 indicating that the model terms are significant and values more than 0.100 suggesting that the regression model is insignificant. The value

of *F* for COD in the current investigation is 366.86, suggesting that the estimated model is significant. In addition, the high values of the response regression coefficients indicate that the model is significant and that the modified *R*²-adjusted value is satisfactory. According to the ANOVA findings, these models indicated the efficiency of the electrocoagulation method and that it could be utilized to remove contaminants from oily wastewater.

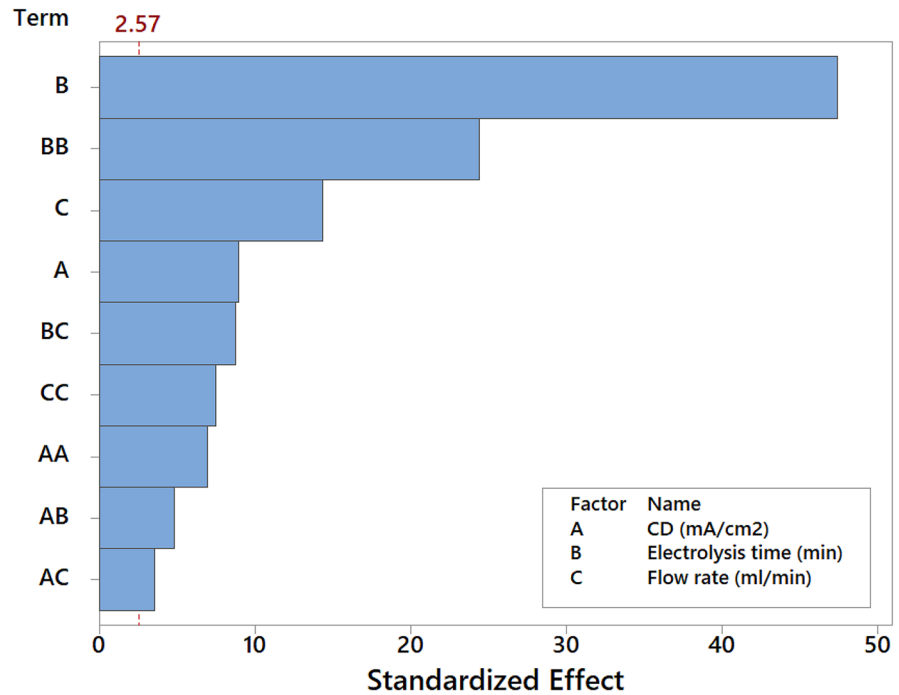
The influences of the current density

This is the most significant parameter in electrocoagulation since it controls pollutant removal rate, ion release from electrodes, and electro coagulant production (Jiang et al., 2019; Mohammed & AlJaberi, 2018). This parameter was adjusted among 0.630 and 5.000 mA/cm² to explore the current density’s effect on the current reactor’s performance (voltage raised from 1.49 to 5.54 V). Figure 7 depicts the relationship between COD removal efficiency and current density at mean reaction time (32 min) and flow rate (100 ml/min). The results reveal that the COD removal effectiveness

Table 6 Mathematical models of the investigated responses

Responses	Mathematical correlations	R ² (adjusted)	R ²
Chemical oxygen demand	$Y_{\text{COD}\%} = -42.67 + 10.08 X_1 + 3.040 X_2 + 0.5919 X_3 - 1.253 X_1^2 - 0.02683 X_2^2 - 0.002590 X_3^2 + 0.0656 X_1 X_2 - 0.02722 X_1 X_3 - 0.005168 X_2 X_3$ (12)	0.9958	0.9985

Fig. 6 Pareto chart for COD removal efficiency



increased from 48.41% at 0.630 mA/cm² to approximately 63.56% at 5.000 mA/cm², resulting in a decrease in the final COD concentration in the treated water from 681 to 481 mg/l. According to the findings, removal efficiency improved as the current density value increased. The finned structure of the anode provides an adequate amount of adsorbent for cleaning the solution (AlJaberi, 2020). An excessively high rate of bubble generation at both electrodes and

the growth of an oxide layer on the electrode reduce the destabilizing pollutant rate and removal efficiency, decreasing this behavior (AlJaberi, 2018; Hansen et al., 2019).

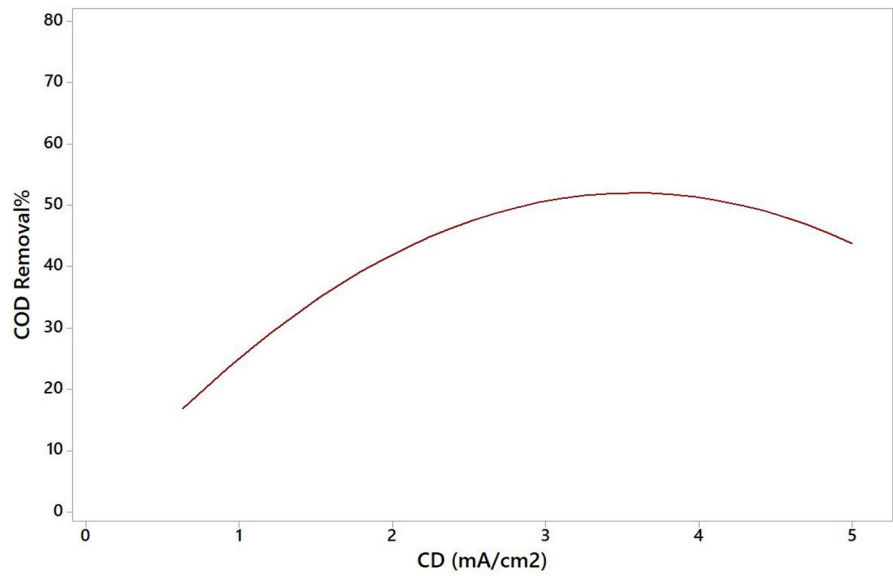
The mathematical relation between COD removal response and current density for mean values of other variables is depicted in Eq. 12 below:

$$Y_{\text{COD}\%} = 29.12 X_1 - 4.075 X_1^2 \quad (R^2 = 71.5\%) \tag{12}$$

Table 7 Results of ANOVA test for COD removal efficiency

Source	Degree of freedom	Sum of squares	Mean square	F-value	P-value
COD removal					
Model	9	9027.13	1003.01	366.86	<0.0001 highly significant
X_1	1	220.98	220.98	80.82	<0.0001 highly significant
X_2	1	6150.41	6150.41	2249.55	<0.0001 highly significant
X_3	1	564.43	564.43	206.44	<0.0001 highly significant
X_1^2	1	132.11	132.11	48.32	0.001 significant
X_2^2	1	1634.29	1634.29	597.75	<0.0001 highly significant
X_3^2	1	154.76	154.76	56.60	0.001 significant
$X_1 * X_2$	1	64.49	64.49	23.59	0.005 significant
$X_1 * X_3$	1	35.37	35.37	12.94	0.016
$X_2 * X_3$	1	209.37	209.37	76.58	<0.0001 highly significant

Fig. 7 The influence of current density on COD removal effectiveness in actual oily wastewater with a COD of 1320 ppm ($\text{mg}_{\text{COD}}/\text{l}$) (electrolysis time = 32 min and flow rate = 100 rpm)



Effect of electrolysis time

Reaction time is an essential operational feature that directly impacts electrocoagulation reactor performance (Changmai et al., 2019). Creating enough electro-coagulants, $\text{Al}(\text{OH})_3$, for adsorption-based pollutant removal from oily wastewater requires some time. Thus, it is essential to look at how long the treatment process takes (AlJaberi et al., 2020). At mean current density and flow rate values of $2.815 \text{ mA}/\text{cm}^2$ and $100 \text{ ml}/\text{min}$, it is clear that the response of COD removal efficiency

increases rapidly with increasing electrolysis time, as shown in Fig. 8. When the response surpasses the mean value of the electrolysis period, hydrogen bubbles at the cathode may interfere with pollutant electro-deposition, causing the response to fall until the experiment’s conclusion (Ahmed et al., 2020). Furthermore, as shown in Eqs. 7 and 8, electrolysis time influences electrode value and energy consumption (Arellano et al., 2020).

Concerning the mean values of other variables, the mathematical relation of COD elimination response versus electrolysis time is indicated in Eq. 13 as follows:

Fig. 8 The impact of electrolysis time on the removal efficiency of COD 1320 ppm ($\text{mg}_{\text{COD}}/\text{L}$) real oily wastewater (current density = $2.815 \text{ mA}/\text{cm}^2$ and flow rate = $100 \text{ ml}/\text{min}$)

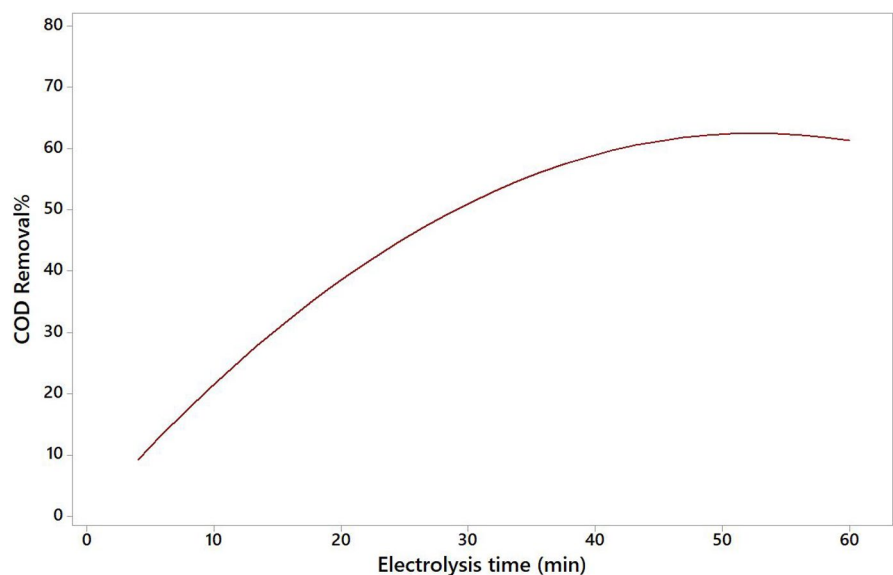
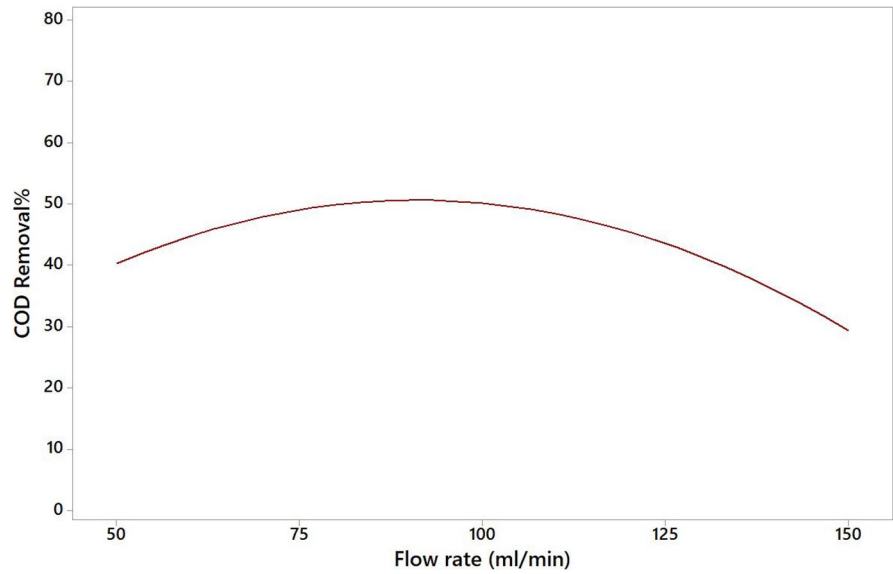


Fig. 9 Flow rate influences COD 1320 ppm (mg_{COD}/l) removal efficiency in real oily wastewater (electrolysis time = 32 min and current density = 2.815 mA/cm²)



$$Y_{\text{COD}\%} = 2.379 X_2 - 0.02262 X_2^2 \quad (R^2 = 96.1\%) \quad (13)$$

As shown in Fig. 8, increasing the reaction duration from 4 to 60 min raised COD removal effectiveness

from 10 to over 60% when using the current innovative electrocoagulation reactor. Since additional adsorption and desorption activities occur during prolonged electrolysis, the removal efficiency of these

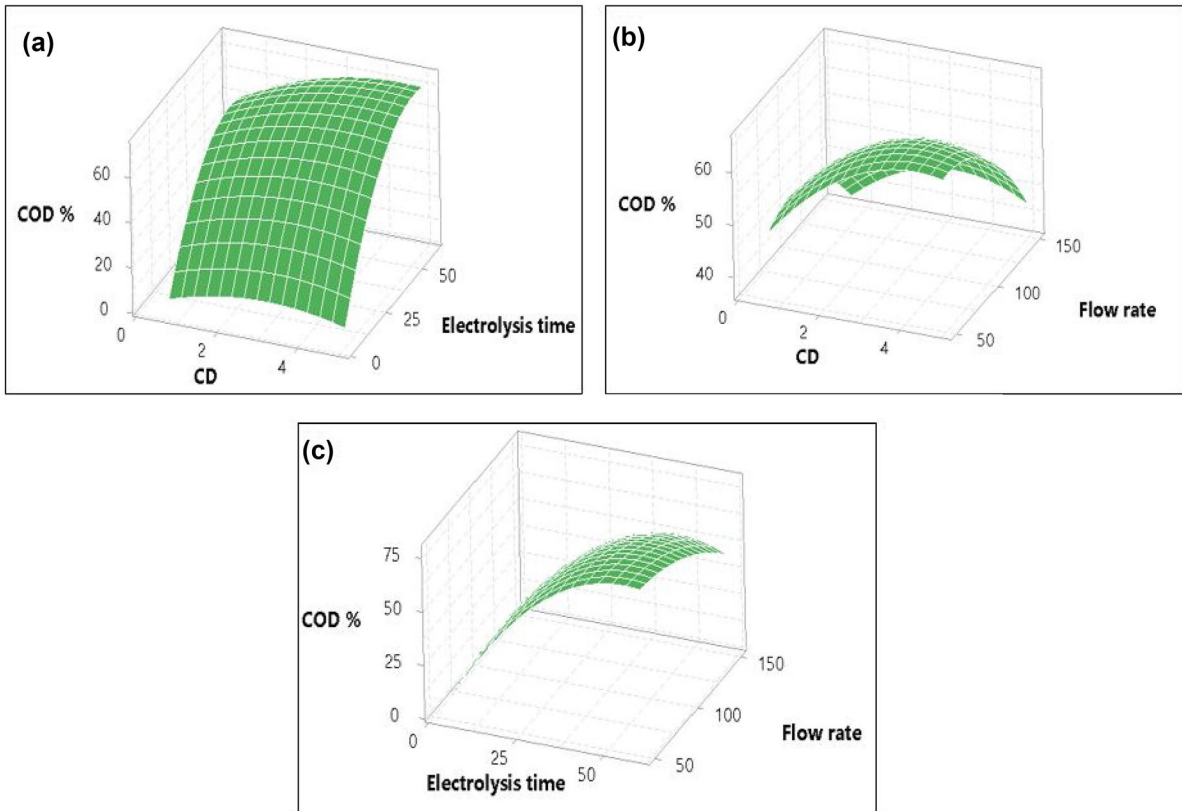


Fig. 10 The influence of each pair of the operating variables on the effectiveness of removing COD from actual oily wastewater. **a** Current density-electrolysis time pair, **b** current density-flow rate pair, and **c** electrolysis time-flow rate pair

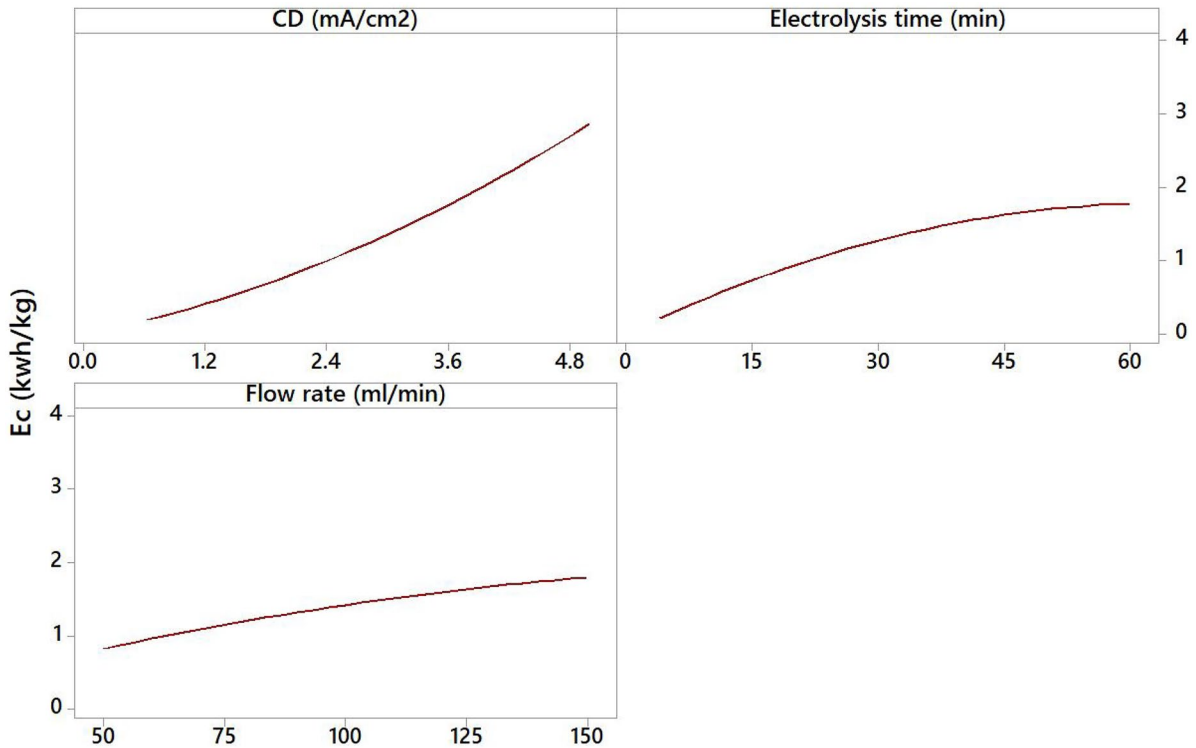


Fig. 11 The relationship between the electrical energy consumption (EEC) and operational factors during the electrocoagulation treatment of COD 1320 ppm (mg_{COD}/l) actual oily wastewater

contaminants from the contaminated solution also increases with reaction time (AlJaberi et al., 2020).

The influence of the flow rate

Since the current design of electrodes featured a tubular-shaped anode and a finny-shaped cathode, the flow rate was chosen as an operating variable and ranged from 50 to 150 ml/min. The results for COD elimination efficiency are shown in Fig. 9 for the mean electrolysis time (32 min) and current density (2.815 mA/cm²). As seen, the response’s behavior as the flow rate changes. It has grown at low flow rates until they reach the mean value. However, it tends to decrease at high flow rates. This could be interpreted at low rates of flow, raising the flow raises the amount of coagulant generation, which raises the removal process; however, at high rates of flow, raising the rate of flow decreases the residence time of the substance inside the reactor (the occurrence of the bypass passage process), and it also rises the incidence of vortices between the electrodes, which diminishes the destabilization process between the atoms

inside the reactor. This result is identical to AlJaberi et al. (2020) and Yang et al. (2021).

The mathematical correlation of COD removal response against the flow rate in regard to mean values of other variables is displayed in Eq. 14 as follows:

$$Y_{\text{COD}\%} = 1.112 X_3 - 0.00611 X_2^3 \quad (R^2 = 75.5\%) \tag{14}$$

Figure 10 depicts the significant impact of every couple of process variables on the effectiveness of COD removal, in which each couple is changed according to the designed range, and the remaining variable is held constant at the mean value, i.e., 2.815 mA/cm² of current density, 32 min of electrolysis time, and 100 ml/min of flow rate, for each situation. The 3D plot of the COD% response indicated that the electrolysis time-flow rate pair has a stronger impact than the current density-electrolysis time couple and the current density-flow rate couple. These findings matched those gained by the ANOVA test, as shown in Table 7. The greatest removal is obtained when the influence of this

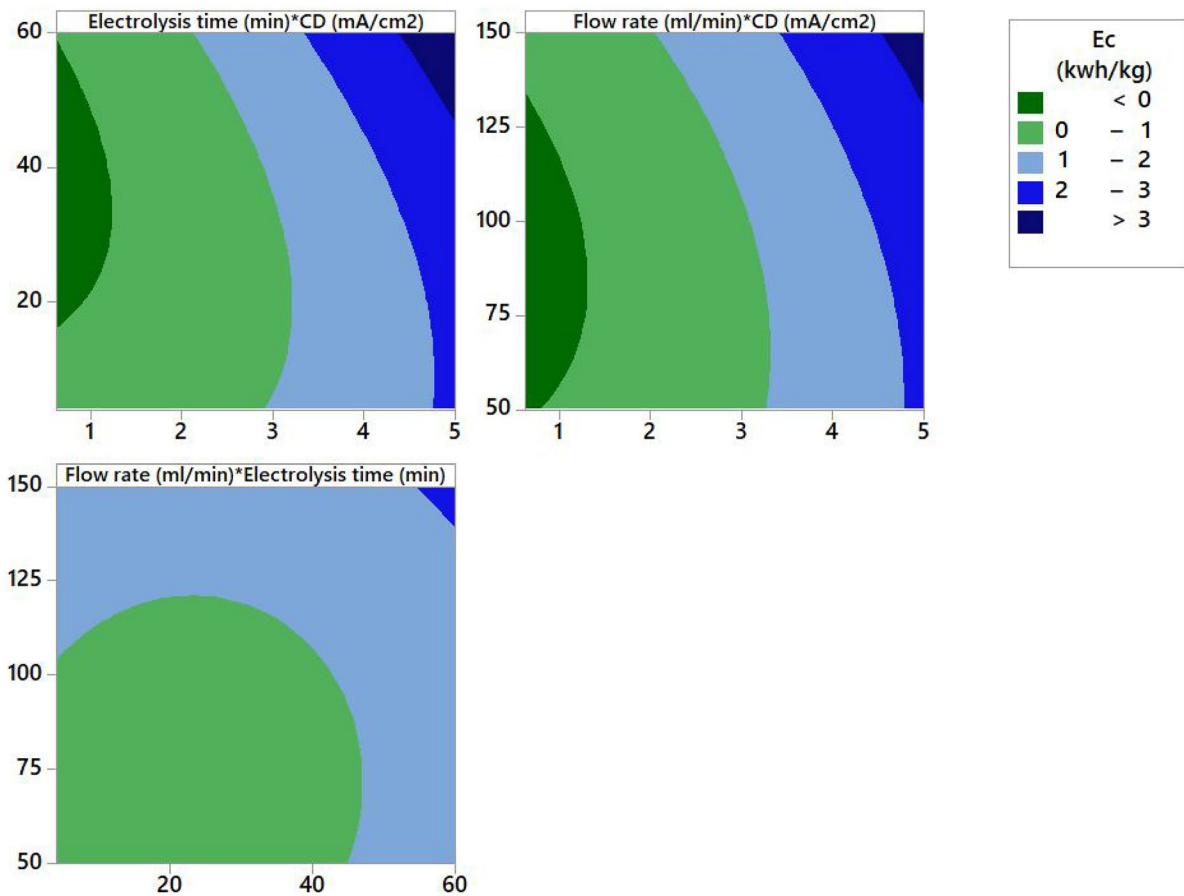


Fig. 12 Electrical energy consumption (EEC) response vs. the contour plots of the studied variables

couple of electrolysis period flow rate is at 1 h and 50 ml/min, whereas the current density electrolysis period couple has at 1 h and 5 mA/cm² and a couple of the flow rate and current density at 50 ml/min and 5 mA/cm².

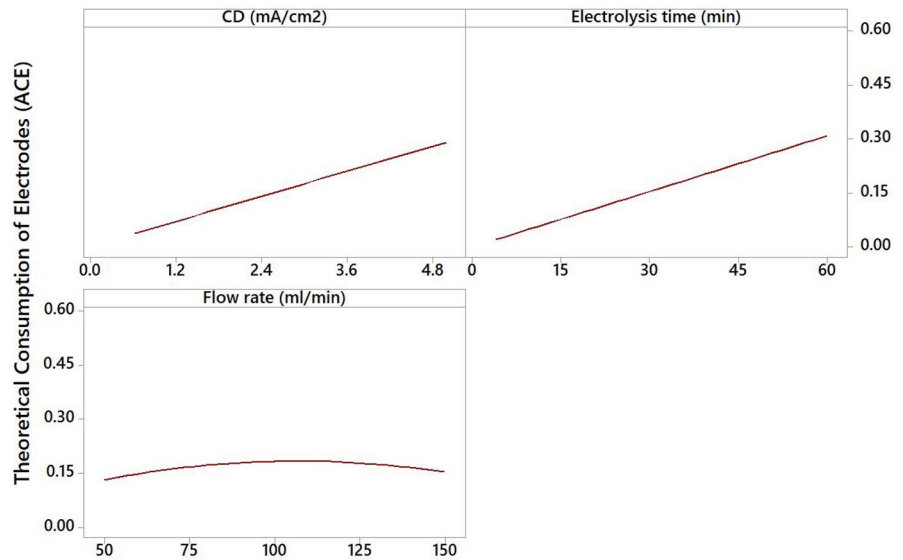
Consumption of electrodes and electrical energy

The electrical energy consumption (EEC), theoretical consumption of electrodes (TCE), and actual consumption of electrodes (ACE) were estimated for the analyzed variables using Eqs. 7, 8, and 9 as illustrated in Figs. 11, 12, 13, and 14. In contrast to TCE, which is directly relevant to the electrolysis time and current density but exhibits different behavior with flow rate, the EEC is typically directly relevant to the electrolysis time, current density, and flow rate. The response of (TCE) increased with increasing flow rate until it

was more than the mean value (100 ml/min), and then it tended to decrease. In the case of ACE, the reaction time correlates directly with the electrolysis time. However, its behavior changes with the current density and flow rate. The response of (ACE) increased with current density, and the flow rate increased until they exceeded the mean value (2.815 mA/cm² and 100 ml/min, respectively), at which point they tended to decrease. At that point, they tend to reduce. The progressive increase and reduction in consumption might be explained by the active area offered by the revolutionary electrode's current design and the electrical conductivity of oily wastewater. The lowest energy usage was 0.11 kWh/kg_{COD}, 0.036 g theoretical electrode consumption, and 0.1 g actual electrode consumption.

The significant effect of each couple of process variables on the electrical energy exhaustion response is depicted in Fig. 12, in which each couple is adjusted

Fig. 13 Electrocoagulation treatment of actual oily wastewater with a COD of 1320 ppm ($\text{mg}_{\text{COD}}/\text{l}$): theoretical consumption of electrodes (TCE) vs the operational factors



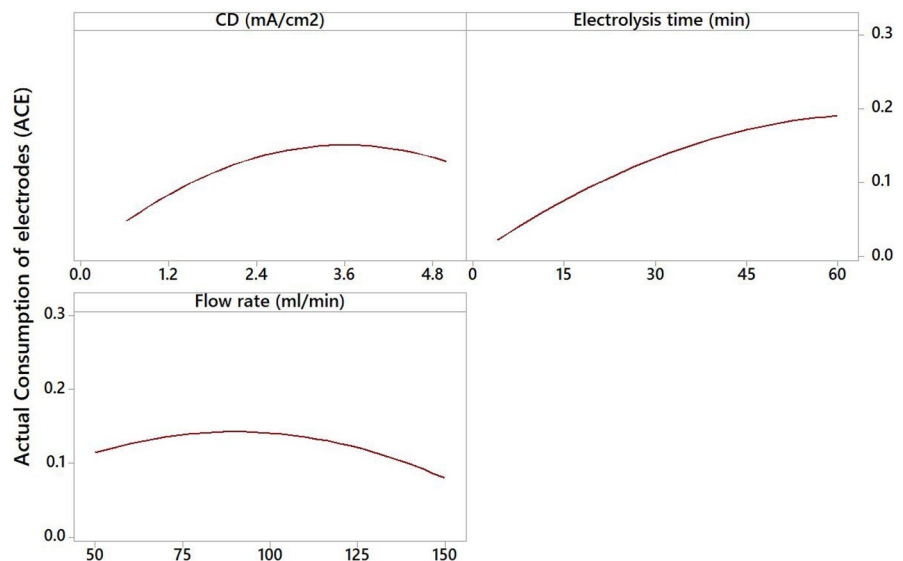
within the selected limits while the other variable is kept constant at the mean value. The current density-flow rate and the current density-electrolysis time couples have a bigger impact than the electrolysis time-flow rate couple, according to the contour plots of the electrical energy exhaustion response.

The irregular interplay between each couple of these parameters, illustrated in Fig. 15, may affect this variation in behavior between factors on response of (ACE) all along study, such as current density and flow rate on the one side and electrolysis time and flow rate on the other side.

The mathematical correlations (Eqs. 16, 17, and 18) in Table 8 were created based on experimental findings and demonstrate the interactions between the operational variables in terms of actual parameters to determine the electrical energy consumption (EEC), theoretical consumption of electrodes (TCE), and actual consumption of electrodes (ACE).

Table 9 summarizes previous studies that addressed the use of electrocoagulation technology in the wastewater treatment process that includes various contaminants.

Fig. 14 Actual consumption of electrodes (ACE) compared to the operational factors during the electrocoagulation treatment of COD 1320 ppm ($\text{mg}_{\text{COD}}/\text{l}$) natural oily wastewater



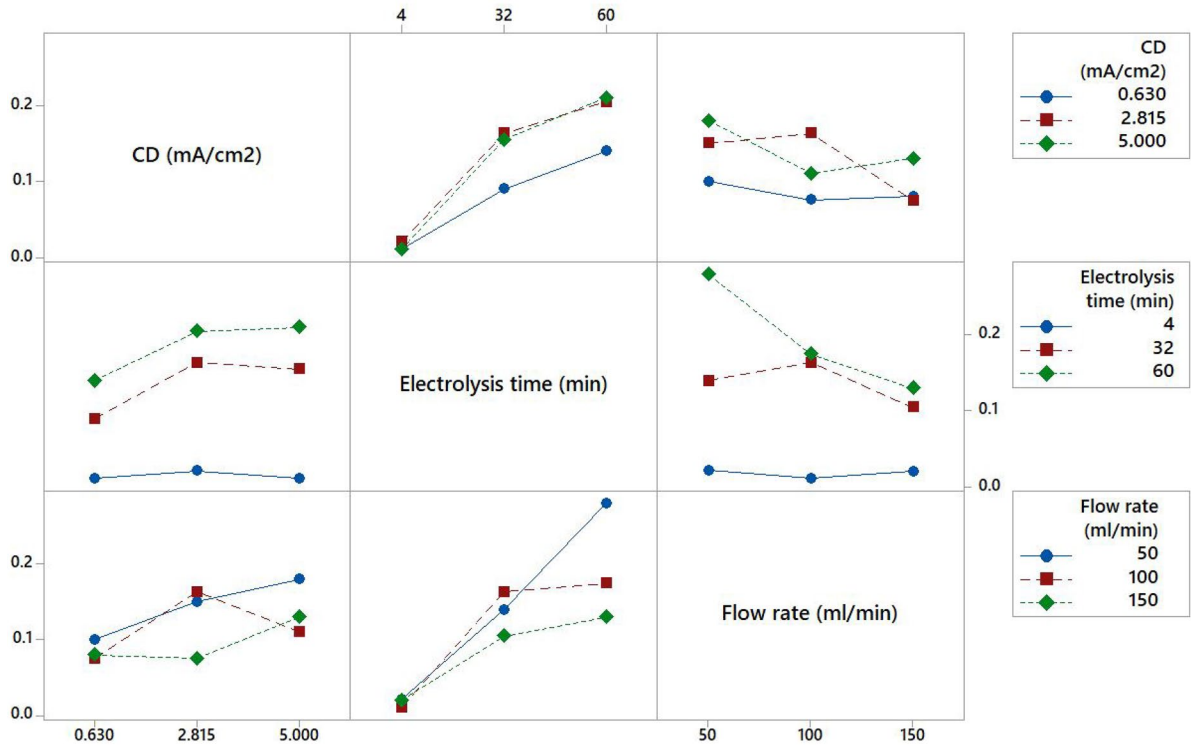


Fig. 15 Actual consumption of electrodes (ACE) response vs. the interaction among the operational variables

Operating parameter optimization

The study’s major findings suggested that the novel design of the electrocoagulation reactor used to recover COD from oily wastewater was treatable. A statistical software application (Minitab-18) was used to estimate the optimization procedure. Figure 16 shows the precision of the findings obtained since the composite desirability (*D*) equals 1. The ideal electrolysis time, current

density, and flow rate were 57.74 min, 5.000 mA/cm², and 50 ml/min, respectively, achieving 82.8% COD elimination efficiency. Because fins offered a greater surface area, the ideal values of the operational variables were smaller than in the past study, especially electrolysis duration and current density. The chemical oxygen demand was reduced by 82.8% at the optimum operational variable values.

Table 8 Mathematical models of the electrical energy consumption (EEC), theoretical consumption of electrodes (TCE), and actual consumption of electrodes (ACE)

Responses	Mathematical correlations	R ² (adjusted)	R ²
The electrical energy consumption (EEC)	$E_c \text{ (kWh/kg)} = 1.562 - 0.214 X_1 - 0.0426 X_2 - 0.0236 X_3 + 0.0636 X_1^2 + 0.000545 X_2^2 + 0.000128 X_3^2 + 0.00751 X_1 * X_2 + 0.00237 X_1 * X_3 - 0.000031 X_2 * X_3 \text{ (16)}$	0.9792	0.9417
Theoretical consumption of electrodes (TCE)	$\text{Theoretical consumption (g)} = -0.00028 + 0.00027 X_1 - 0.000196 X_2 + 0.000064 X_3 - 0.000100 X_1^2 + 0.000000 X_2^2 - 0.000001 X_3^3 + 0.001819 X_1 * X_2 + 0.000000 X_1 * X_3 + 0.000002 X_2 * X_3 \text{ (17)}$	0.9999	0.9998
Actual consumption of electrodes (ACE)	$AEC = -0.1366 + 0.0449 X_1 + 0.00824 X_2 + 0.001336 X_3 - 0.00634 X_1^2 - 0.000051 X_2^2 - 0.000004 X_3^2 + 0.000286 X_1 * X_2 - 0.000069 X_1 * X_3 - 0.000027 X_2 * X_3 \text{ (18)}$	0.9827	0.9514

Table 9 Summarizes previous studies of electrocoagulation technology

References	Pollutants	Anode metal	Cathode metal	Optimum parameter values	Efficiency
Ibrahim et al. (2011)	COD	Mild steel	Stainless steel	3 A/dm ² , 60 min, pH 7	93.51%
Ghanim (2014)	COD	Fe	Fe	20 mA/cm ² , 56.54 min, pH 7	85.7538%
Shokri (2018a)	COD	Al	Al	16 mA/cm ² , 14.2 min, pH 8	88.3%
Shokri (2018b)	COD	Fe	Fe	40 mA/cm ² , 60 min, pH 9	91.70%
Shokri (2019)	COD	Al	Al	2 mA/cm ² , 60 min, pH 7	85.5%
Shokri and Karimi (2020)	COD	Pt	Carbon	0.7 A, 30 min, pH 10	69%

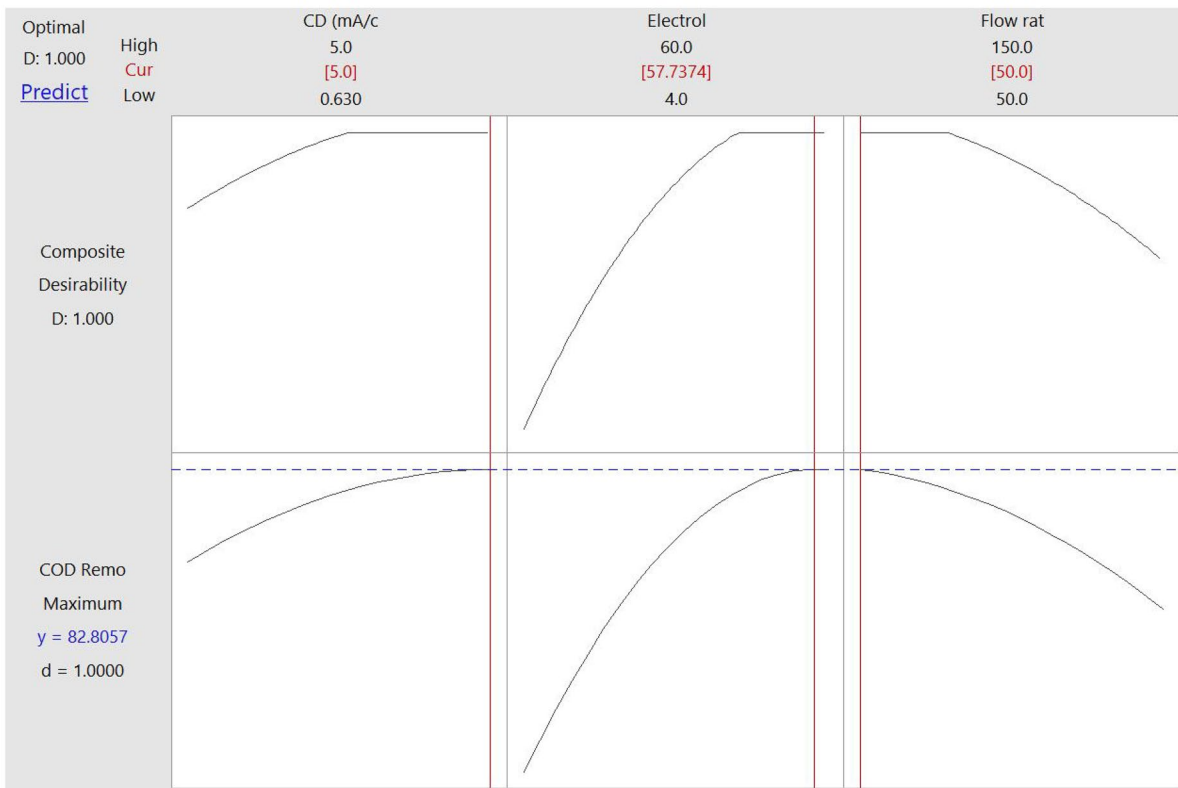


Fig. 16 The ideal operational variable settings and investigated responses for the treatment of COD 1320 ppm (mg_{COD}/l) actual oily wastewater

As shown in Fig. 16, the lowest flow rate was the desired value because any increase in this parameter increases the discharge of untreated solution due to a decrease in the residence time of the solution in the reactor, which affects the needed interaction between the ions in the solution. At the same time, a more excellent value of current density and electrolysis time would be beneficial to assure the release of various ions essential for the synthesis of electro-coagulants.

Conclusion

The performance of a new electrocoagulation reactor (ECR) in eliminating COD from Al-Muthanna petroleum refinery effluent was investigated. The electrolysis period, current density, and flow rate were determined to be best at 60 min, 5 mA/cm², and 50 ml/min, respectively. COD elimination efficiency was 82% (the concentration of chemical oxygen demand was reduced

from 1320 to 232 mg/L) under these conditions. Additionally, an energy consumption of 4.787 (kWh/kg_{COD}) and an electrode consumption of 0.544 (g) were found. As previously stated, current density significantly impacts COD removal, followed by electrolysis time. Increasing the flow rate had a negative influence on COD removal efficiency. The analyses of data ANOVA and the higher regression coefficients indicate that the second-order polynomial model had been adjusted desirably. To determine the impact count of the operational variables on the studied answers, Pareto charts were used. As a rule of thumb, the oxidation process is faster than the reduction process throughout the electrochemical cell, which means that the release of aluminum ions from the anode is much than the release of hydroxyl ions at the cathode; therefore, we need to maximize the surface area of the cathode without excessive enlargement of the reactor's volume. This study found the solution to this challenge through the use of fins at the cathode's surface with a significantly small wet volume of the reactor. As a result, the amount of hydroxyl ions has been increased, more electro-coagulants are generated incorporated with aluminum ions, and consequently higher removal efficiency of pollutants is attained. Overall, the outcomes of the study demonstrated that the new design of the electrocoagulation reactor is reliable for the purgation of natural oily wastewater.

Acknowledgements The authors express their gratitude to Al-Muthanna Petroleum Refinery, The Laboratory of Al-Muthanna Sewer Directorate.

Author contribution Muhammad Aiyd Jasim and Forat Yasir AlJaberi were responsible by carrying out of experiments, data interpretations, and manuscript writing. All authors reviewed the manuscript.

Availability statement Data is available upon reasonable request.

Declarations

Ethical approval All authors have read, understood, and have complied as applicable with the statement on "Ethical responsibilities of Authors" as found in the Instructions for Authors and are aware that with minor exceptions, no changes can be made to authorship once the paper is submitted.

Conflict of interest The authors declare no competing interests.

References

- Ahmed, S.A., AlJaberi, F.Y., & Makki, H.F. (2020). Electrocoagulation treatment of high saline oily wastewater: evaluation and optimization. *Heliyon*, 6, e03988.
- AlJaberi, F. Y. (2018). Studies of autocatalytic electrocoagulation reactor for lead removal from simulated wastewater. *Journal of Environmental Chemical Engineering*, 5, 6069–6078.
- AlJaberi, F. Y. (2019). Modelling current efficiency and ohmic potential drop in an innovated electrocoagulation reactor. *Desalination and Water Treatment*, 164, 102–110.
- AlJaberi, F.Y. (2020). Removal of TOC from oily wastewater by electrocoagulation technology. *IOP Conference Series: Materials Science and Engineering*, 928, 022024.
- AlJaberi, F. Y., Abdulmajeed, B. A., Hassan, A. A., & Ghadban, M. L. (2020). Assessment of an electrocoagulation reactor for the removal of oil content and turbidity from real oily wastewater using response surface method. *Recent Innovations in Chemical Engineering*, 13, 55–71.
- Almukdad, A., Hawari, A. H., & Hafiz, M. A. (2021). An enhanced electrocoagulation process for the removal of Fe and Mn from municipal wastewater using dielectrophoresis. *Water*, 13(4), 485.
- Al-Zuheri, H. A., & Mohammed, T. J. (2018). Application of response surface methodology for analysis and optimization of the operational parameters for turbidity removal from oily wastewater by electrocoagulation process. *IOP Conference Series: Materials Science and Engineering*, 454, 1–13.
- Arellano, M., Oturan, N., Pazos, M., Sanromán, M. A., & Oturan, M. A. (2020). Coupling electro-Fenton process to a biological treatment, a new methodology for the removal of ionic liquids. *Separation and Purification Technology*, 233, 115990.
- Barzega, G., Wu, J., & Ghanbari, F. (2019). Enhanced treatment of greywater using electrocoagulation/ozonation: Investigation of process parameters. *Process Safety and Environmental Protection*, 121(1), 125–132.
- Changmai, M., Pasawan, M., & Purkait, M. K. (2019). Treatment of oily wastewater from drilling site using electrocoagulation followed by microfiltration. *Separation and Purification Technology*, 210, 463–472.
- Cheng, X., & Gong, Y. (2018). Treatment of oily wastewater from cold-rolling mill through coagulation and integrated membrane processes. *Environmental Engineering Research*, 23, 159–163.
- De Carvalho, H. P., Huang, J., Zhao, M., Liu, G., Dong, L., & Liu, X. (2015). Improvement of methylene blue removal by electrocoagulation/banana peel adsorption coupling in a batch system. *Alexandria Engineering Journal*, 54(3), 777–786.
- Ghanbari, F., & Moradi, M. (2016). Electrooxidation processes for dye degradation and colored wastewater treatment from: Advanced nanomaterials for wastewater remediation. *CRC Press*, 3, 61–108.
- Ghanim, A. N. (2014). Optimization of pollutants removal from textile wastewater by electrocoagulation through RSM. *Journal of Babylon University/engineering Sciences*, 22(2), 375–387.

- Hansen, H. K., Peña, S. F., Gutiérrez, C., Lazo, A., & Ottosen, L. M. (2019). Selenium removal from petroleum refinery wastewater using an electrocoagulation technique. *Journal of Hazardous Materials*, *364*, 78–81.
- Hassan, A. A., Naeema, H. T., & Hadi, R. T. (2018). Degradation of oily wastewater in aqueous phase using solar (ZnO, TiO₂ and Al₂O₃) catalysts. *Pakistan Journal of Biotechnology*, *15*(4), 909–916.
- Ibrahim, D. S., Sakthipriya, N., & Subramanian, B. (2011). Electro-coagulation treatment of oily wastewater with sludge analysis. *Water Science & Technology*, *5*, 17–24.
- Jabbar, S. M., AlJaberi, F. Y., & Jabbar, N. M. (2020). Modeling of adsorption isotherms of oil content through the electrocoagulation treatment of real oily wastewater. *AIP Conference Proceedings*, *2213*, 020041.
- Jain, S. K., & Singh, V. P. (2003). Water quality modeling. *Developments in Water Science*, *51*, 743–786.
- Jiang, W. m., Chen, Y. m., Liu, M. C., Liu, X. l., Wang, Y. T., & Yang, J. (2019). Removal of emulsified oil from polymer-flooding sewage by an integrated apparatus including EC and separation process. *Separation Purification Technology*, *211*, 259–268.
- Mohammed, W. T., & AlJaberi, F. Y. (2018). Novel method for electrocoagulation removal of lead from simulated wastewater by using concentric tubes electrodes reactor. *Desalination and Water Treatment*, *111*, 86–91.
- Mohammed, W. T., & AlJaberi, F. Y. (2021). The most practical treatment methods for wastewaters: A systematic review. *Mesopotamia Environmental Journal*, *5*(1), 1–28.
- Mokif, L. A., Jasim, H. K., & Abdulhusain, N. A. (2022). Petroleum and oily wastewater treatment methods: a mini review. *Materials Today: Proceedings*, *49*, 2671–2674.
- Mustapha, H. I. (2018). *Treatment of petroleum refinery wastewater with constructed wetlands*. CRC Press.
- Papadopoulos, K. P., Argyriou, R., & Economou, C. N. (2019). Economou, Treatment of printing ink wastewater using electrocoagulation. *Journal of Environmental Management*, *237*(1), 442–448.
- Schaep, J., Bruggen, B. V., Uytterhoeven, S., Croux, R., Vandecasteele, C., Wilms, D., & Houtte, E. V. (1998). Removal of hardness from groundwater by nanofiltration. *Desalination*, *119*(1–3), 295–301.
- Shokri, A. (2018a). Employing electrocoagulation for the removal of acid red 182 in aqueous environment by using Box-Behnen design method. *Desalination and Water Treatment*, *115*, 281–287.
- Shokri, A. (2018b). The treatment of spent caustic in the wastewater of olefin units by ozonation followed by electrocoagulation process. *Desalination and Water Treatment*, *111*, 173–182.
- Shokri, A. (2019). Application of electrocoagulation process for the removal of acid orange 5 in synthetic wastewater. *Journal of Chemistry and Chemical Engineering*, *38*(2), 113–119.
- Shokri, A., & Karimi, S. (2020). Treatment of aqueous solution containing acid red 14 using an electro peroxone process and a Box-Behnken experimental design. *Archives of Hygiene Sciences*, *9*, 48–57.
- Yang, S., Sun, J., Wu, K., & Hu, C. (2021). Enhanced oil droplet aggregation and demulsification by increasing electric field in electrocoagulation. *Chemosphere*, *283*, 131123.

Publisher's Note Springer Nature remains neutral with regard to jurisdictional claims in published maps and institutional affiliations.

Springer Nature or its licensor (e.g. a society or other partner) holds exclusive rights to this article under a publishing agreement with the author(s) or other rightsholder(s); author self-archiving of the accepted manuscript version of this article is solely governed by the terms of such publishing agreement and applicable law.